



Hepatic stellate cells retain the capacity to synthesize retinyl esters and to store neutral lipids in small lipid droplets in the absence of LRAT

Mokrish Ajat^{1,2}, Martijn Molenaar¹, Jos F.H.M. Brouwers, Arie B. Vaandrager, Martin Houweling, J. Bernd Helms^{*}

Department of Biochemistry & Cell Biology, Faculty of Veterinary Medicine, and Institute of Biomembranes, Utrecht University, P.O. Box 80176, 3508 TD Utrecht, The Netherlands

ARTICLE INFO

Article history:

Received 24 June 2016

Received in revised form 7 October 2016

Accepted 28 October 2016

Available online 1 November 2016

Keywords:

Hepatic stellate cells

LRAT

DGAT1

Retinyl esters

Lipid droplets

Lipidomics

ABSTRACT

Hepatic stellate cells (HSCs) play an important role in liver physiology and under healthy conditions they have a quiescent and lipid-storing phenotype. Upon liver injury, HSCs are activated and rapidly lose their retinyl ester-containing lipid droplets. To investigate the role of lecithin:retinol acyltransferase (LRAT) and acyl-CoA:diacylglycerol acyltransferase 1 (DGAT1) in retinyl ester synthesis and lipid droplet dynamics, we modified LC–MS/MS procedures by including multiple reaction monitoring allowing unambiguous identification and quantification of all major retinyl ester species. Quiescent primary HSCs contain predominantly retinyl palmitate. Exogenous fatty acids are a major determinant in the retinyl ester species synthesized by activated HSCs and LX-2 cells, indicating that HSCs shift their retinyl ester synthesizing capacity from LRAT to DGAT1 during activation. Quiescent LRAT^{−/−} HSCs retain the capacity to synthesize retinyl esters and to store neutral lipids in lipid droplets ex vivo. The median lipid droplet size in LRAT^{−/−} HSCs (1080 nm) is significantly smaller than in wild type HSCs (1618 nm). This is a consequence of an altered lipid droplet size distribution with 50.5 ± 9.0% small (≤700 nm) lipid droplets in LRAT^{−/−} HSCs and 25.6 ± 1.4% large (1400–2100 nm) lipid droplets in wild type HSC cells. Upon prolonged (24 h) incubation, the amounts of small (≤700 nm) lipid droplets strongly increased both in wild type and in LRAT^{−/−} HSCs, indicating a dynamic behavior in both cell types. The absence of retinyl esters and reduced number of lipid droplets in LRAT-deficient HSCs in vivo will be discussed.

© 2016 Elsevier B.V. All rights reserved.

1. Introduction

Retinoids (vitamin A and its derivatives) are important compounds for embryonic development and are involved in many cellular processes such as proliferation, differentiation and vision [1–3]. Vitamin A is an essential nutrient and storage is important to warrant sufficient supply of retinoids in times of insufficient acquisition from the diet. The liver has the largest capacity to store retinol as retinyl esters. Approximately 70–90% of the retinyl esters are stored in lipid droplets of hepatic stellate cells [1,4–8].

Abbreviations: ARAT, acyl coenzyme A:retinol acyltransferase; DGAT1, acyl-CoA:diacylglycerol acyltransferase 1; HSC, hepatic stellate cell; LRAT, lecithin:retinol acyltransferase; MRM, multiple reaction monitoring; PC, phosphatidylcholine; TAG, triacylglycerol.

^{*} Corresponding author. Department of Biochemistry and Cell Biology, Utrecht University, P.O. Box 80176, 3508 TD Utrecht, The Netherlands.

E-mail address: j.b.helms@uu.nl (J.B. Helms).

¹ These authors contributed equally to this work.

² Current address: Department of Veterinary Preclinical Sciences, Faculty of Veterinary Medicine, Universiti Putra Malaysia, 43400 UPM Serdang, Selangor, Malaysia.

Two enzymatic activities have been implicated in the acylation of retinol resulting in the formation of retinyl esters. Lecithin:retinol acyltransferase (LRAT) catalyzes a trans-esterification reaction that occurs between retinol and phosphatidylcholine (PC), transferring the fatty acid at the *sn*-1 position of PC to retinol [9–11]. LRAT does not have a clear preference for physiologically occurring fatty acids at the *sn*-1 position of PC [12]. The other enzymatic activity catalyzes an acyl coenzyme A:retinol acyltransferase (ARAT) reaction. Acyl-CoA:diacylglycerol acyltransferase 1 (DGAT1), one of the enzymes involved in triacylglycerol synthesis, has been shown to possess ARAT activity [13–15]. LRAT and DGAT1 are both expressed in liver and their contribution to retinyl ester synthesis and storage has been subject to investigations. LRAT-deficient mice have only trace levels of retinyl esters in the liver, both in the presence of physiological or elevated dietary doses of retinol [16]. Moreover, retinyl ester concentrations in livers from DGAT-deficient mice are similar to those reported in wild type livers [15,17]. Therefore, LRAT is believed to account for the major if not only enzymatic activity involved in liver retinyl ester formation. Hence, the predominant retinyl ester species found in HSC lipid droplets is retinyl palmitate followed by retinyl stearate and retinyl oleate, in order of abundance [48]. This retinyl ester species preference likely reflects the abundance of the fatty acid moiety at the *sn*-1 position of PC. DGAT1 can act as a physiologically important ARAT in

mouse intestine, e.g. in the absence of LRAT or in the presence of elevated retinoid concentrations [17]. In addition, DGAT1 is essential for retinoid homeostasis in the skin [18].

Most if not all cells have the capacity to retain and accumulate neutral lipids such as triacylglycerols and cholesteryl esters in lipid droplets [19–21]. In lipid droplets of HSCs, the concentration of retinyl esters makes up 13–60% of the neutral lipids, depending largely on the dietary retinoid supply [22,23]. HSCs in LRAT knockout mice lack retinyl esters and appear morphologically normal. Surprisingly, in addition to an absence of retinyl esters, HSCs lack their characteristic lipid droplets [13], implying that the synthesis and storage of retinyl esters is essential for the presence of lipid droplets in HSCs.

Upon liver injury, HSCs are activated and trans-differentiate into proliferative and fibrogenic myofibroblasts. Activated HSCs are key players in the development of hepatic fibrosis and cirrhosis as the source of extracellular matrix synthesis [22,24]. During activation, HSCs lose their large lipid droplets in a highly dynamic and regulated process [25–27]. The reasons for the loss of lipid droplets during HSC activation are not known as LRAT-deficient HSCs have a quiescent phenotype but lack lipid droplets [13]. The aim of this study was to investigate retinyl ester synthesis and lipid droplet formation in HSCs in the absence of LRAT. For this, we made use of two different conditions. First, we studied retinyl ester formation in LX-2 cells that resemble the activated HSC phenotype [28]. Second, we studied retinyl ester formation and lipid droplet dynamics in quiescent primary HSCs lacking LRAT. We show that LRAT-deficient hepatic stellate cells retain the capacity to synthesize retinyl esters and to generate lipid droplets.

2. Materials and methods

2.1. Materials

Dulbecco's modified Eagle's medium (DMEM), fetal bovine serum (FBS), penicillin-streptomycin and Fungizone were purchased from Gibco (Paisley, UK). The human hepatic stellate cell line (LX-2) was kindly donated by Dr. Friedman (New York, NY, USA). Oleic acid, palmitic acid, cholesterol, vitamin A standards and butylated hydroxytoluene were obtained from Sigma-Aldrich (St. Louis, MO, USA). All-*trans*-retinol was prepared in ethanol (10 mM), retinyl acetate and palmitate in chloroform:methanol (1:1). Stock concentrations were verified by UV-spectrophotometry. Cell culture dishes and 4-wells plates were from Nunc (Roskilde, Denmark). Deuterated palmitate ($\text{CH}_3(\text{CH}_2)_7(\text{CD}_2)_2(\text{CH}_2)_5\text{COOH}$) and oleate ($\text{CH}_3(\text{CH}_2)_7\text{CD}=\text{CD}(\text{CH}_2)_7\text{COOH}$) were purchased from Cambridge Isotope Laboratories (Andover, MA, USA). Solvents used for extraction and chromatography (all HPLC/MS grade) were obtained from Roth (Karlsruhe, Germany) and BioSolve (Valkenswaard, The Netherlands). Fermentas 2 × Taq PCR master mix from Thermo Fisher Scientific (Waltham, MA, USA), RNeasy mini kit from Qiagen (Venlo, The Netherlands) and the iScript cDNA synthesis kit from Bio-Rad (Hercules, CA, USA). BCA protein determination kit was from Pierce (Rockford, IL, USA). For fluorescence microscopy, LD540 was kindly donated by Dr. C. Thiele, Bonn, Germany. BODIPY 493/503, goat-anti-mouse-alexa647 and donkey-a-rabbit-alexa647 were purchased at Life Technologies (Paisley, UK). RNAiMAX was from Invitrogen (Paisley, UK). Antibodies against desmin and α -SMA were from Thermo Scientific (Waltham, MA, USA). Paraformaldehyde (8%) was obtained from Electron Microscopy Sciences (Hatfield, PA, USA).

2.2. Methods

2.2.1. Ethics statement

Mice were treated according to the governmental and international guidelines on animal experimentation, and were approved by the Dutch Animal Experimental Licensing Committee (DEC).

2.2.2. Cell culture and preparation of fatty acid-albumin complexes

The human-derived hepatic stellate cell line LX-2 [28] was cultured in DMEM medium supplemented with 10% FBS, 100 units/ml penicillin, 100 $\mu\text{g}/\text{ml}$ streptomycin and 4 $\mu\text{l}/\text{ml}$ Fungizone. All cells were maintained in a humidified 5% CO_2 incubator at 37 °C and sub-cultured once a week. Fatty acids were complexed to fatty-acid free BSA (10 mM fatty acid, 2 mM BSA) according to standard procedures and stored at –20 °C. BSA was made fatty acid free as described [51].

2.2.3. Isolation of primary liver cells

LRAT gene knockout mouse strain was generated as described previously and generously provided by Dr. L. Gudas [29]. Disruption of the LRAT gene by targeted replacement of exon 1 with a loxP-flanked neo gene cassette was confirmed by PCR (62 °C annealing temperature, 72 °C reaction temperature) using the following primers: LRAT upstream: 5'-TCTGGCATCTCTCTACGCTG-3'; LRAT WT-reverse: 5'-CATTAGATGGGCGACAC-GGT-3'; LRAT KO-reverse: 5'-TTGAAGACGAAAGG GCCTCG-3'. All mice were fed a standard chow diet containing 15 IU retinol/g. Primary hepatocytes and hepatic stellate cells (HSCs) were isolated from wild type and LRAT^{–/–} mice by collagenase digestion followed by differential centrifugation [30]. After isolation, HSCs and hepatocytes were plated in 35 mm dishes in DMEM supplemented with 10% fetal bovine serum (FBS), 100-units/ml penicillin and 100 $\mu\text{g}/\text{ml}$ streptomycin and 4 $\mu\text{l}/\text{ml}$ Fungizone. HSC contamination in hepatocyte fractions was routinely assessed by immunofluorescence with antibodies against desmin (see Confocal microscopy). On average, $3.1 \pm 1.9\%$ of cells in this fraction was scored as desmin-positive. Retinyl ester determination in these fractions is expressed relative to the amount of cholesterol. The hepatic stellate cell fraction was found to contain 7.64 ± 1.17 nmol cholesterol/ 10^6 cells. For the hepatocyte fraction this level is 99.0 ± 13.4 nmol cholesterol/ 10^6 cells.

2.2.4. Formation of deuterated lipids in cultured cells

Cells were plated in triplicate in 6 cm dishes and grown in DMEM containing 10% FBS until 60–70% confluency. Incubations were started by replacing the growth medium with DMEM/10% FBS supplemented with retinol (8 μM) and in the absence or presence of (deuterated) (D_4 -) palmitate and/or (D_2 -) oleate (80 μM). At indicated time points, incubations were stopped by removing the medium and washing the cells twice with ice-cold PBS. Subsequently cells were collected and stored at –20 °C until further analysis. Aliquots were used for lipid analysis as described below.

2.2.5. Extraction of retinoids and neutral lipids

Samples were extracted in the dark under red light. Cell aliquots were homogenized by sonication (10 s, 5 μm amplitude) and 800 μl of cell homogenate was transferred to an amber glass tube, 1 nmol of retinyl acetate in MeOH/ CHCl_3 (1:1, v/v) was added (internal standard) together with 10 nmol butylated-hydroxytoluene to avoid photo isomerization of the retinoids. Lipids were extracted as described by Ref. [31]. The combined chloroform phases were evaporated to dryness in amber tubes under the stream of N_2 and stored at –20 °C until further analysis.

2.2.6. Neutral lipid analysis by HPLC–MS/MS

Before analysis, samples were dissolved in MeOH/ CHCl_3 (1:1) and kept in amber vials at 4 °C. Lipid separation was performed on a 250×3.0 mm Synergi™ 4u Max-RP 80A column (4 μm particle size, Phenomenex, CO, USA) at a flow rate of 350 $\mu\text{l}/\text{min}$ with a gradient of acetonitrile:water (95:5, solvent A) to acetone:chloroform (85:15, solvent B) using the following linear gradients between all time points (time in min, % solvent A): (0, 90%), (5, 40%), (17, 0%), (19, 90%), and (25, 90%). The gradient was generated by a Flexar UHPLC system (Perkin Elmer, Waltham, MA, USA). The column effluent was analyzed by triple quadrupole mass spectrometry (API 4000 QTRAP, MDS Sciex/Applied Biosystems, Foster City, Canada) using atmospheric pressure chemical ionization (APCI) as ionization source. Source temperature

was set at 500 °C. Multiple reaction monitoring (MRM) in positive ion mode was used to detect retinol, retinyl acetate and (deuterated) retinyl esters by monitoring the transition from m/z 269.2 to m/z 93.1. Molecule specific transitions as described in Table 1 were used for the detection of cholesterol, (deuterated) retinyl ester species and (deuterated) triacylglycerol species. Cholesterol was determined by monitoring the transition from m/z 369.3 to m/z 287.3 during MRM analysis of retinyl esters (Table 1). Of note: due to the ionization source, triacylglycerol species are fragmented mostly to diacylglycerol species, which are distinguished from endogenous diacylglycerol species by lipid separation (UHPLC) prior to mass spectrometry analysis. Elution of retinyl ester species was determined by the m/z signals in MRM mode (Table 1). Quantification of retinyl ester species was based on the m/z 269.2 signal, which is species independent. In the case of overlapping peaks, the peak ratios of the MRM transitions were used to determine the relative contribution of each retinyl ester. In these cases, the response factor differed only marginally because of similar fatty acid compositions. The response factor of retinyl palmitate was used for quantification of the m/z signals in MRM mode. Retinyl acetate was added prior to lipid extraction as an internal standard to correct for lipid extraction recovery.

Integration of chromatographic peaks and quantification was performed using Analyst software version 1.4.3 (Applied Biosystems, Foster City, Canada).

For LX-2 cells, retinyl ester quantitation was expressed as pmol retinyl ester/mg protein. For primary HSCs, retinyl ester quantitation was expressed as pmol retinyl ester/nmol cholesterol.

2.2.7. Antisense oligonucleotide treatment of LX-2 cells

LX-2 cells were seeded in antibiotics-free medium on 6-wells plates and treated with premixed siRNA pools from Dharmacon ON-TARGET siRNA Smartpool (Thermo Fisher Scientific, Waltham, MA, USA) and RNAiMAX (Invitrogen) complexes. For DGAT1, a Smartpool of siRNAs complementary to the following target sequences was used: 5'-CUUG

AGCAAUGCCCGGUA-3', 5'-CAAUAGCCGUCCUCAUGUA-3', 5'-UCAA GGACAUGGACUACUC-3', and 5'-GCUGUGGUCUUACUGGUUG-3'. For DGAT2, a Smartpool of siRNAs complementary to the following target sequences was used: 5'-GAACACACCAAGAAAGGU-3', 5'-GGAGGU AUCUGCCUGUCA-3', 5'-UCAUGGAGCUGACCUGGUU-3', and 5'-GAAU GCCUGUGUUGAGGGA-3'. As a control, a non-target siRNA pool with random sequences was used. Knockdown was performed with 8 pmol siRNA pool and 5 μ l RNAiMAX per well. After 24 h, the medium was refreshed with complete medium containing antibiotics. 72 h after transfection cells were incubated with retinol and deuterated fatty acids for MS-analysis (see previous section) or washed twice and scraped in ice-cold PBS for RT-PCR analysis.

2.2.8. Semiquantitative RT-PCR analysis

Total RNA was isolated from cell homogenates using a Qiagen RNeasy Mini kit and cDNA was synthesized with a Bio-Rad iScript cDNA Synthesis kit, both according to the manufacturer's protocol. RT-PCR was performed with Fermentas 2 \times Taq PCR master mix, 30 ng of cDNA and 160 nM of sense and antisense primer in a final volume of 50 μ l. Primers for human DGAT1 were 5'-GGCCTTCTCCACGAGTACC-3' (sense) and 5'-GGCCTCATAGTTGAG CACG-3' (antisense). Primers for human DGAT2 were 5' ATCACCAGTGTGTGGAGA-3' (sense) and 5'-CAGACACCATGACACTTCC-3' (antisense) as described before [52]. Primers for human Gapdh were 5' CTCCTCTGTTCGACAGTCA-3' (sense) and 5' GATCTCGCTCTGGAAGATG-3' (antisense) and designed to be positive for cDNA and negative for genomic DNA. PCR products from various numbers of cycles were separated on a 2% agarose gel and visualized with ethidium bromide and UV. The bands were imaged with a Bio-Rad Gel Doc XR imaging system.

2.2.9. Confocal microscopy

HSCs and hepatocytes were plated onto glass cover slips in 4-well plates and incubated overnight or for 7 days in DMEM supplemented

Table 1
MRM-transitions of HPLC-MS/MS.

Analyte	Q1 (m/z)	Q3 (m/z)	Dwell time (ms)	Declustering potential (V)	Collision energy (V)
Retinol, retinyl esters	269.2	93.1	100	50	33
Retinol-D5, retinyl-D5 esters	274.2	93.1	100	50	33
Cholesterol, cholesteryl esters	369.3	287.3	20	80	27
Retinyl acetate (C2:0)	329.2	269.2	150	75	26
Retinyl myristate (C14:0)	497.4	269.2	150	75	26
Retinyl palmitoleate (C16:1)	523.4	269.2	150	75	26
Retinyl palmitate (C16:0)	525.5	269.2	150	75	26
Retinyl-D5 palmitate (C16:0)	530.5	274.2	150	75	26
Retinyl palmitate-D4 (C16:0-D4)	529.5	269.2	150	75	26
Retinyl linolenate (C18:3)	547.5	269.2	150	75	26
Retinyl linoleate (C18:2)	549.5	269.2	150	75	26
Retinyl oleate (C18:1)	551.5	269.2	150	75	26
Retinyl-D5 oleate (C18:1)	556.5	274.2	150	75	26
Retinyl stearate (C18:0), -oleate-D2 (C18:1-D2)	553.5	269.2	150	75	26
Retinyl-D5 stearate (C18:0)	558.5	274.2	150	75	26
Retinyl eicosapentaenoate (C20:5)	571.6	269.2	150	75	26
Retinyl-D5 arachidonate (C20:4)	578.6	274.2	150	75	26
Retinyl arachidonate (C20:4)	573.6	269.2	150	75	26
Retinyl dihomo- γ -linolenate (C20:3)	575.5	269.2	150	75	26
Retinyl docosahexaenoate (C22:6)	597.6	269.2	150	75	26
Retinyl docosapentaenoate (C22:5)	599.6	269.2	150	75	26
DAG (18:1/18:1), TAG (18:1/18:1/X)	603.5	264.3	20	75	30
DAG (18:1-D2 [*] /18:1), TAG (18:1-D2 [*] /18:1/X)	605.5	264.3	20	75	30
DAG (18:1-D2 [*] /18:1-D2 [*]), TAG (18:1-D2 [*] /18:1-D2 [*] /X)	607.5	266.3	20	75	30
DAG (16:0/18:1), TAG (16:0/18:1/X)	577.5	264.3	20	75	30
DAG (16:0/18:1-D2 [*]), TAG (16:0/18:1-D2 [*] /X)	579.5	266.3	20	75	30
DAG (16:0-D4/18:1), TAG (16:0-D4/18:1/X)	581.5	264.3	20	75	30
DAG (16:0-D4/18:1-D2 [*]), TAG (16:0-D4/18:1-D2 [*] /X)	583.5	266.3	20	75	30
DAG (16:0/16:0), TAG (16:0/16:0/X)	551.5	238.3	20	75	30
DAG (16:0-D4/16:0), TAG (16:0-D4/16:0/X)	555.5	242.3	20	75	30
DAG (16:0-D4/16:0-D4), TAG (16:0-D4/16:0-D4/X)	559.5	242.3	20	75	30

* 18:1-D2 or 18:0 share the same mass, but can be distinguished by retention time.

with 10% FBS, 100-units/ml penicillin and 100 µg/ml streptomycin and 4 µl/ml Fungizone. Samples were fixed in 4% paraformaldehyde, permeabilized and blocked for 60 min with 2% BSA/0.1% saponin in PBS, incubated for 60 min with antibodies against desmin or α -SMA in 1% BSA/0.1% saponin, washed four times in PBS and stained with donkey-anti-rabbit-alexa647 (desmin) or goat-anti-mouse-alexa647 (α -SMA) in combination with BODIPY and DAPI (1% BSA/0.1% saponin) for 60 min. After four washing steps with PBS, coverslips were mounted onto an object glass with FluorSave and analyzed using a Leica TCS SP2 Laser Scanning Spectral Confocal Microscope (Germany) with preset settings for the representative dyes. Images were analyzed with CellProfiler v2.1.1.

For visualization of vitamin A positive lipid droplets, cells were plated onto glass cover slips in 4-well plates and incubated for various times in DMEM supplemented with 0.5% FBS, 100-units/ml penicillin and 100 µg/ml streptomycin and 4 µl/ml Fungizone. Samples were fixed in 4% paraformaldehyde, washed two times in PBS and stained with LD-dye LD540 [32] and desmin as described above. Mounted slides were imaged using a Leica TCS SP2 Laser Scanning Spectral Confocal Microscope (Germany) with preset settings for the representative dyes. Auto-fluorescence of retinoids was imaged by 405 nm laser excitation; the emission was detected between 415 and 450 nm.

2.2.10. Other methods

Protein was measured using the BCA protein assay kit, according to the manufacturer's instructions, using BSA as a standard. Results are expressed as mean \pm S.D. or mean \pm SEM. Statistical analyses were performed using a paired or unpaired *t*-test, Mann–Whitney *U* test, or one-way ANOVA.

3. Results

3.1. Lipidomic analysis of retinyl ester formation

Detection and identification of retinyl ester species has strongly improved by coupling HPLC-based separation to mass spectrometric detection [33–35]. Under these conditions, however, it is often difficult to discriminate between closely related retinyl esters such as retinyl palmitate and retinyl oleate because of very similar retention times. We modified current methodologies that combine HPLC separation of neutral lipids with subsequent peak analysis using mass spectrometry by including multiple reaction monitoring (MRM, [Materials and methods](#)). The modified method allows the unambiguous identification and quantitation of most retinyl esters using retinyl acetate as an internal standard. We applied this method to the analysis of retinol containing lipids in the hepatic stellate cell line LX-2 after incubation of these cells with retinol for 24 h ([Fig. 1](#)). The elution profile of all retinol containing lipids was obtained by mass spectroscopy in MRM mode by monitoring the transition from *m/z* 269.2 (backbone of retinol) to *m/z* 93.1 (fragment of retinol, due to retinol-specific fragmentation). The eluate was also analyzed for retinyl ester species-specific mass transitions ([Table 1](#), [Fig. 1B](#)). The most common retinyl esters identified in LX-2 cells include retinyl linoleate, retinyl oleate, retinyl palmitate, retinyl stearate as well as less abundant retinyl esters. As in most other methods, retinyl oleate and retinyl palmitate migrate closely together on HPLC due to their resemblance in hydrophobicity, but they can now be clearly distinguished by tandem mass spectrometry analysis in MRM mode.

3.2. Retinyl ester species in liver, primary HSCs, and LX-2 cells

After incubation of LX-2 cells with retinol, the retinyl ester composition of LX-2 cells was quantified and compared with the retinyl ester composition of mouse liver and primary mouse hepatic stellate cells. Quantification of the retinyl ester profile of LX-2 cells shows a broad variety of retinyl ester species ([Fig. 2A](#)). The major retinyl esters

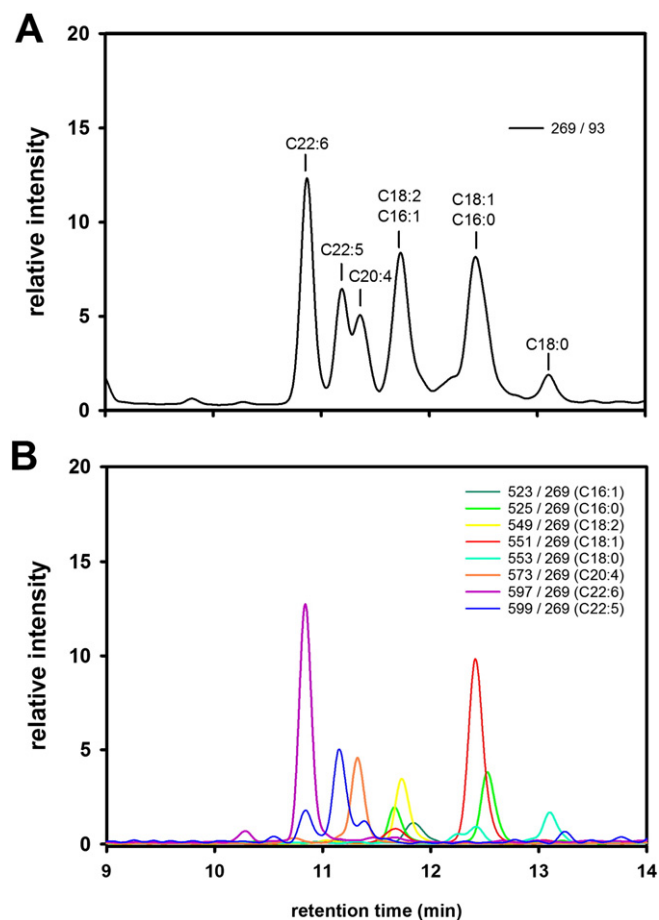


Fig. 1. Retinyl ester determination by HPLC-MS/MS analysis. LX-2 cells were incubated with 5 µM retinol for 24 h and analyzed for the presence of retinyl esters as described in [Materials and methods](#). (A) Elution profile of the MRM-transition 269.2/93.1, characteristic for retinol containing lipids including retinyl esters and free retinol. (B) Overlay of eight MRM transitions (IM + H)/269.2 of the most abundant retinyl esters in LX-2 cells, indicated in the figure. In both panels, signal is expressed relative to the transition (329.2/269.2) of the internal standard retinyl acetate (not shown, retention time 8.1 min). Details of mass spectrometric analysis are described in [Materials and methods](#).

synthesized are retinyl palmitate ($C_{16:0}$), retinyl oleate ($C_{18:1}$), and retinyl docosahexaenoate ($C_{22:6}$). In contrast, the major retinyl ester in total mouse liver ([Fig. 2B](#)) and mouse hepatic stellate cells ([Fig. 2C](#)) is retinyl palmitate. This is in agreement with earlier reports [48,29,13] on the retinyl ester composition of liver and HSCs in various species. Thus, the retinyl ester composition of LX-2 cells is much more diverse as compared to liver and HSCs (cf. [Fig. 2A–C](#)). The diversity in retinyl esters of the LX-2 cells cannot be explained by the 24 h incubation of LX-2 cells in the presence of 10% FBS and retinol, as primary HSCs incubated for 24 h under the same conditions show a comparable retinyl ester profile as HSCs without subsequent incubation for 24 h (cf. [Fig. 2C](#) and D).

These observations point to the presence of a retinol esterification activity in LX-2 cells which is distinct from LRAT, the primary retinyl ester forming enzyme in liver and primary hepatic stellate cells. LRAT has an almost exclusive preference for fatty acids at the *sn*-1 position of PC [53] [9,11]. Given the fact that the seven most abundant PC species in LX-2 cells contained at least one palmitate (together representing 63% of the total PC pool, data not shown), the sole involvement of LRAT in retinyl ester synthesis is unlikely to explain the broad variety of retinyl ester species observed in LX-2 cells. In agreement with this, we find that incubation of LX-2 cells for 24 h with retinol in the presence of exogenous fatty acids stimulates retinyl ester formation and that the exogenously added fatty acid is a significant determinant of the retinyl ester species synthesized ([Suppl. Fig. 1A](#)). This suggests that

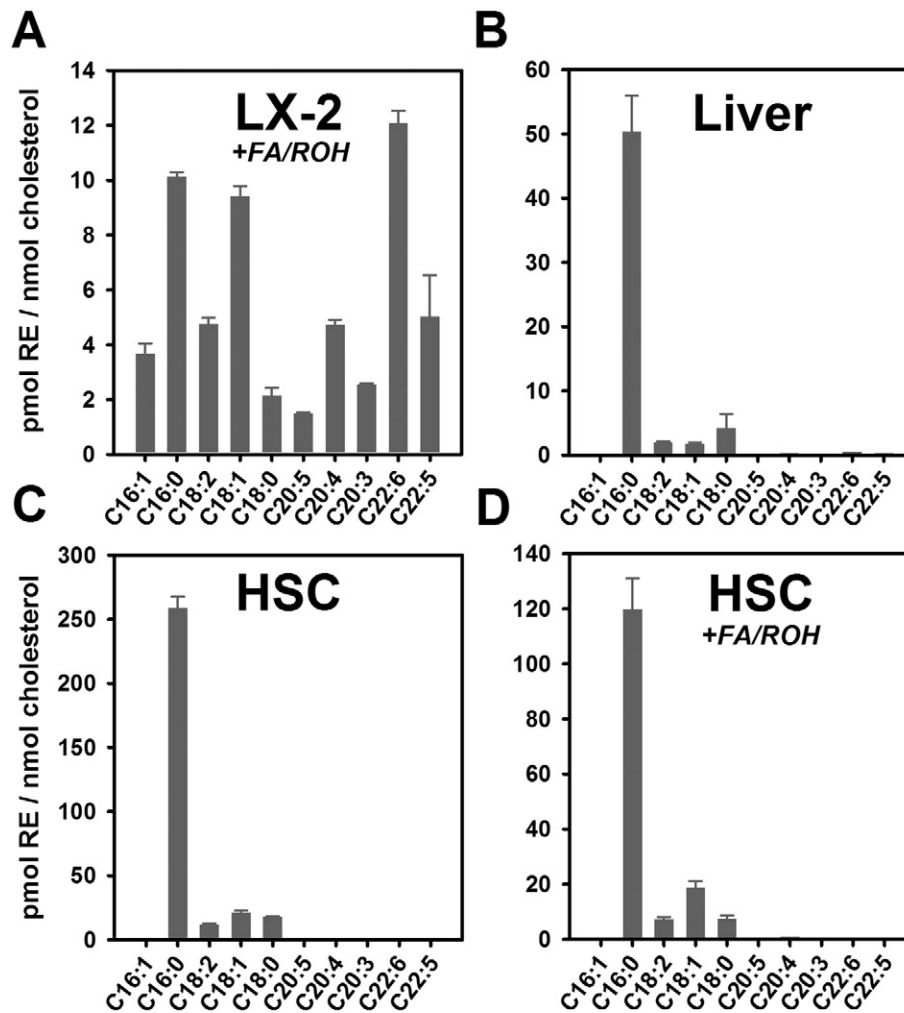


Fig. 2. Retinyl ester composition of liver, hepatic stellate- and LX-2 cells. The retinyl ester composition of LX-2 cells (A), liver (B), HSCs directly after isolation (C) and HSCs after 24 h incubation (D) was analyzed as described in [Materials and methods](#). LX-2 cells (A) and HSCs (D) were incubated for 24 h in DMEM/10% FBS supplemented with 8 μ M retinol prior to retinyl ester analysis. A representative experiment is shown which was repeated at least two times with similar results.

exogenously added fatty acids are at least partly incorporated into retinyl esters by an ARAT activity.

3.3. Involvement of DGAT-1 in retinyl ester synthesis in LX-2 cells

DGAT-1, the final enzyme in triacylglycerol biosynthesis, has ARAT activity [15]. DGAT-2 also catalyzes the formation of TAG from diacylglycerol and acyl-CoA, but no retinol esterification activity has been attributed to this enzyme. To determine the role of DGAT-1 and DGAT-2 in the esterification of retinol and TAG synthesis in LX-2 cells, DGAT-1 and DGAT-2 knockdown experiments were performed using siRNA. Subsequently, LX-2 cells were incubated with retinol and deuterated oleate allowing determination of incorporation of exogenous oleate into retinyl oleate, one of the major retinyl ester species formed in LX-2 cells (Fig. 2). The effect of the knockdown experiments on DGAT-1 and/or DGAT-2 mRNA expression levels indicated a knockdown efficiency of approximately 70% for DGAT-1 and 80% for DGAT-2, relative to glyceraldehyde-3-phosphate dehydrogenase (Fig. 3A). Treatment of LX-2 cells with DGAT-1 silencing oligonucleotides resulted in a 47% ($p < 0.01$) reduction in the incorporation of D₂-oleate into retinyl oleate (Fig. 3B). No significant effect on the incorporation of this deuterated fatty acid in 3 major oleate-containing TAG species was observed (Fig. 3C). The decrease in retinyl oleate synthesis (retinyl D₂-oleate) in the DGAT-1 knockdown cells (Fig. 3B) was accompanied by a comparable reduction ($41.5 \pm 1.5\%$) in the amount of unlabeled retinyl oleate

(Fig. 3D). DGAT-1 knockdown showed a similar reduction of retinyl palmitate synthesis, whereas the synthesis of retinyl esters containing poly-unsaturated fatty acids was inhibited to a lesser extent. Incubation of DGAT-2-silenced LX-2 cells showed different results. The incorporation of D₂-oleate in 3 major TAG species was significantly inhibited (40%; $p < 0.01$, Fig. 3C), with less effect on retinyl ester levels in LX-2 cells as compared to DGAT1 knockdown (Fig. 3D). A double knockdown (DGAT-1 and -2) showed a slightly higher inhibition of both retinyl ester and TAG synthesis when compared to the separate knockdown of DGAT-1 and DGAT-2, respectively. The data from the DGAT-1 and DGAT-2 knockdown experiments reveal that ARAT activity, in particular DGAT-1, contributes significantly to retinol esterification of retinyl palmitate, retinyl oleate and other retinyl esters in LX-2 cells.

3.4. Retinyl ester formation in primary rat hepatic stellate cells

LX-2 cells resemble the activated HSC phenotype in several aspects [28]. Under physiological circumstances, hepatic stellate cells have a quiescent phenotype in a healthy liver with large retinyl ester containing lipid droplets. Upon liver injury, HSCs become activated and trans-differentiate into a myofibroblast phenotype. During this activation process, HSCs lose their characteristic lipid droplets, retinyl esters, and LRAT expression [22,24,25,36,37]. Collectively, our data with LX-2 cells predict that activated HSCs retain the capacity to synthesize REs, but with a different species profile.

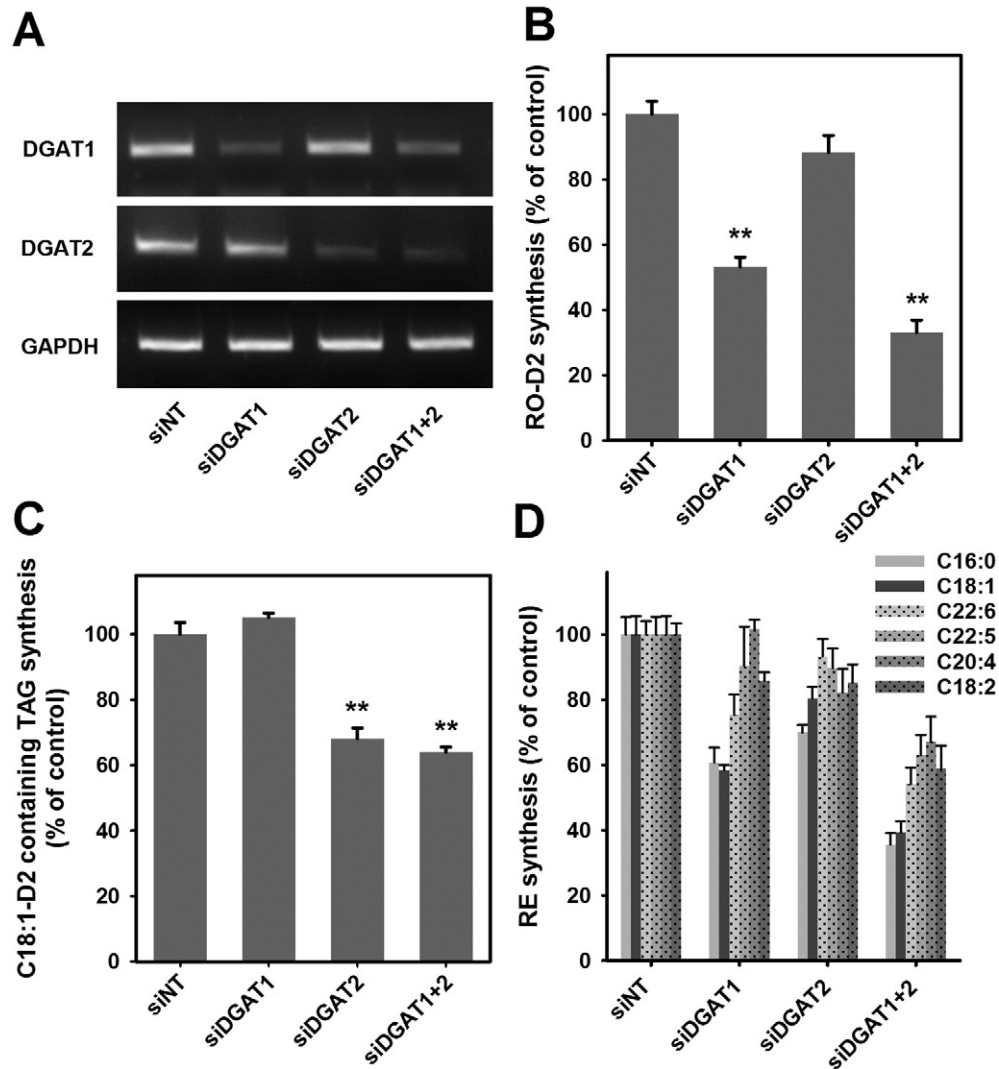


Fig. 3. Effect of DGAT-1 and DGAT-2 knockdown on retinyl ester and triacylglycerol synthesis in LX-2 cells. LX-2 cells were treated for 48 h with antisense oligonucleotides to knockdown DGAT-1 or/and DGAT-2 activity. The efficiency of the knockdown was determined by PCR (A). Subsequently the cells were incubated with 8 μ M retinol and 100 μ M D₂-oleate. After 24 h, the incubations were stopped, cells collected, lipids extracted and retinyl ester (B, D₂-retinyl oleate) and triacylglycerol (C, D₂-oleate containing triacylglycerol species) were quantified using HPLC-MS as described in [Materials and methods](#). The effect of the knockdown of DGAT-1, DGAT-2 or a combination of DGAT-1 and DGAT-2 in LX-2 cells on the six major retinyl ester species is shown in (D). A representative experiment is shown which was repeated at least two times with similar results. Significantly different from control incubations: ** $P < 0.01$.

To investigate this, HSCs were isolated from rat liver and quiescent (day 0) and activated HSCs (day 7) were incubated with or without deuterium labeled retinol for 24 h. Usage of deuterium labeled retinol allowed discrimination of endogenously present retinyl esters, predominantly present in quiescent HSCs, from newly synthesized retinyl esters. Lipids were extracted and retinyl ester content was measured by HPLC-MS/MS in MRM-mode. During the activation process, rat HSCs lose most of their endogenous (unlabeled) retinyl esters (Fig. 4, upper left panel). The retinyl ester species distribution changes from predominantly retinyl palmitate (>80%) to a more diverse species distribution (Fig. 4, lower left panel). This indicates either a preferential breakdown of retinyl palmitate during HSC activation or rapid and unselective breakdown of all retinyl esters and concomitant (increased) synthesis of a larger variety of retinyl esters. Incubation of HSCs with retinol-D5 revealed a difference in the distribution of retinyl ester species that are synthesized in quiescent and activated HSCs. Whereas retinyl palmitate is predominantly synthesized in quiescent HSCs, a larger repertoire of retinyl esters are synthesized in activated HSCs (Fig. 4, right panels). In addition, the retinyl esters synthesizing capacity in activated HSCs (Fig. 4, upper right panel) is larger than the amount of retinyl esters recovered in activated HSCs (Fig. 4, upper left panel), suggesting a high

retinyl ester turnover. These results are in agreement with our previous findings on a highly dynamic turnover of retinyl esters during the HSC activation process [25].

The results obtained show that activated primary rat HSCs behave different from quiescent HSCs and suggest that during activation HSCs switch from LRAT to DGAT1 for their retinyl ester synthesis. To directly study the contribution of LRAT and other enzymes to retinyl ester synthesis in primary quiescent hepatic stellate cells, retinyl ester synthesis was studied in wild type and LRAT knockout mice [29]. The absence of retinyl esters was confirmed in various tissues from LRAT^{-/-} mice whereas retinyl esters were readily detected in various tissues of wild type mice (Suppl. Table 1). The levels of retinyl ester storage are known to vary with retinol concentrations in the diet and the data reported here are in good agreement with reported retinyl ester concentrations in these tissues [13,29]. The absence of LRAT did not affect cholesterol, cholesteryl ester and TAG levels in these tissues. The absence of retinyl esters was also confirmed in primary HSCs and hepatocytes from LRAT^{-/-} mice (Suppl. Fig. 2). Cholesteryl ester and triacylglycerol levels were less affected by the absence of LRAT in HSCs, as demonstrated by a 1.4 fold reduction of cholesteryl esters and a 2.9 fold reduction of triacylglycerols (Suppl. Fig. 2).

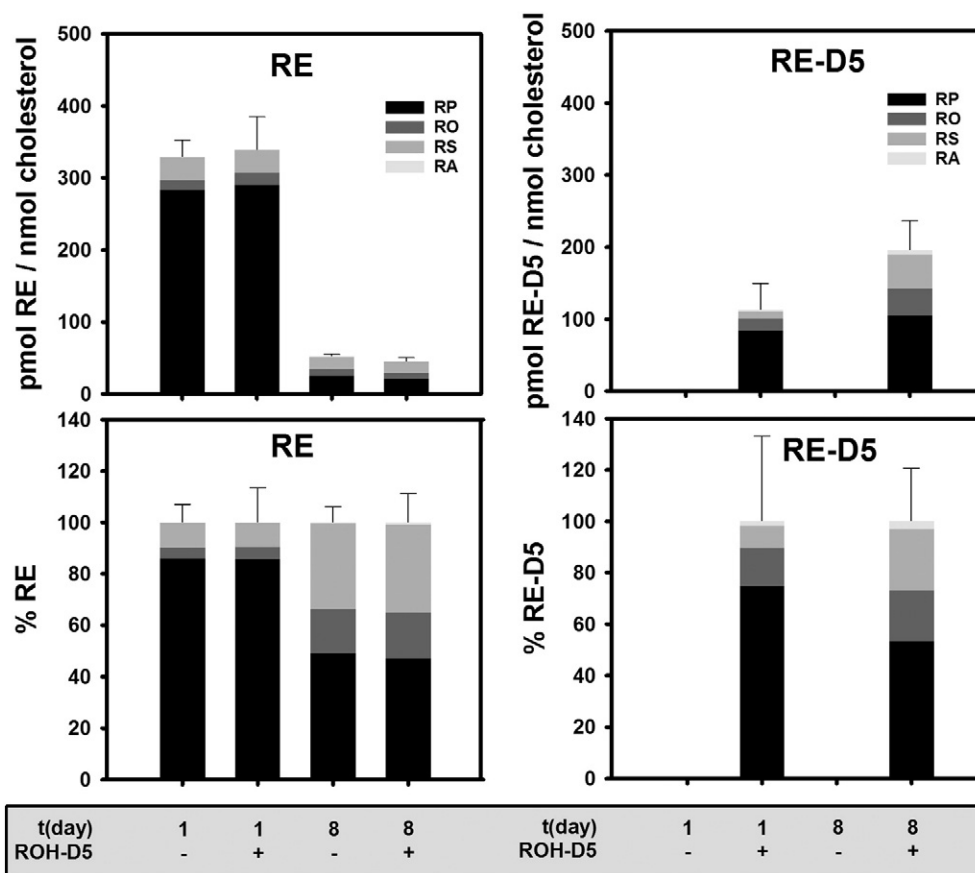


Fig. 4. Retinyl ester synthesis in quiescent and activated primary rat hepatic stellate cells. Primary rat hepatic stellate cells were incubated at day 0 or day 7 with or without 10 μ M retinol-D5 for 24 h. Lipids were extracted and retinyl ester content was measured by HPLC–MS/MS in MRM-mode (Table 1). Left panels: quantitation of unlabeled (endogenous) retinyl palmitate (RP, black), retinyl oleate (RO, dark grey), retinyl stearate (RS, grey) and retinyl arachidonate (RA, light grey). Right panels: quantitation of total amount of labeled retinyl-D5 palmitate, retinyl-D5 stearate and retinyl-D5 arachidonate. Data were normalized by total free cholesterol as determined by MRM transition 369/287 (upper panels) or expressed as a percentage of the total RE-pool (lower panels). Results represent the means \pm standard deviation of triplicates of a representative experiment ($n = 3$).

To investigate the capacity of quiescent HSCs isolated from $LRAT^{-/-}$ mice to synthesize retinyl esters, HSCs from wild type and $LRAT^{-/-}$ mice were incubated with retinol (8 μ M) and the deuterated fatty acids D_4 -palmitate and D_2 -oleate (80 μ M each). Fig. 5A shows that HSCs from $LRAT^{-/-}$ mice are able to synthesize retinyl esters, although to a much lesser extent as compared to HSCs from wild type mice. As $LRAT$ is not present in HSC from $LRAT^{-/-}$ knockout mice, retinyl esters must be synthesized by an alternative pathway, most likely involving $DGAT1$ activity. $LRAT$ and $DGAT1$ have different substrate affinities, resulting in a different spectrum of retinyl ester species. In agreement with the involvement of $DGAT1$, the median D_4 -retinyl palmitate percentage \pm SEM of the total labeled retinyl ester pool (D_4 -palmitate + D_2 -oleate retinyl esters) shifted from $83 \pm 4\%$ in HSC cell of control mice to $55 \pm 8\%$ in HSC of $LRAT^{-/-}$ mice ($p < 0.05$, one-way ANOVA, Fig. 5B).

Hepatocytes have a much lower capacity to synthesize retinyl esters as compared to HSCs (13 pmol RE/nmol cholesterol in hepatocytes versus 59 pmol RE/nmol cholesterol in wild type HSCs). In addition, in hepatocytes the D_4 -retinyl palmitate percentage of the total labeled retinyl ester pool (D_4 -palmitate + D_2 -oleate retinyl esters) is less affected by the absence ($63 \pm 5\%$, $p < 0.05$) or presence ($70 \pm 1\%$, $p < 0.01$) of $LRAT$. Both values are also well below the observed $83 \pm 4\%$ in HSCs of control mice (Fig. 5B).

3.5. TAG synthesis in HSCs and hepatocytes of $LRAT^{-/-}$ and wild type mice

HSCs have the highest retinyl ester storage (Suppl. Fig. 2) and $LRAT$ activity (Fig. 5), but they also have the most pronounced reduction in the

amounts of the other stored neutral lipids upon deletion of the $LRAT$ gene (Suppl. Fig. 2). These results suggest a possible link between retinyl ester and TAG synthesis, in agreement with morphological observations describing an absence of lipid droplets in $LRAT$ -deficient HSCs [13]. We therefore investigated the effect of $LRAT$ gene deletion on TAG synthesis. HSCs and hepatocytes from wild type and $LRAT^{-/-}$ mice were incubated with a mixture of the deuterated fatty acids (D_4 -palmitate and D_2 -oleate, each 80 μ M) and retinol. In the absence of $LRAT$, TAG synthesis of species with two deuterated fatty acids is 36% lower as compared to HSCs from wild type mice (Fig. 6A). Comparable results were obtained with TAG species containing one and three deuterated fatty acids (data not shown). Thus, the presence of $LRAT$ enzyme does affect TAG synthesis but only to a modest extent. Similar results were obtained in the hepatocyte fraction (Fig. 6B). In both cell types, the absence of $LRAT$ did not affect the TAG species distribution (Fig. 6C and D).

3.6. Lipid droplet formation in HSCs from $LRAT^{-/-}$ mice

HSCs from $LRAT^{-/-}$ mice do contain TAGs (Suppl. Fig. 2) and have the capacity to synthesize retinyl esters (Fig. 5) and TAGs (Fig. 6). These observations seem to contrast morphological observations describing the absence of lipid droplets in HSCs of $LRAT^{-/-}$ mice [13]. The presence of lipid droplets in primary HSCs was therefore studied by confocal microscopy using desmin as a marker protein for HSCs and the lipophilic dye LD540 to identify lipid droplets [32]. The presence of retinyl esters in lipid droplets was determined by auto-fluorescence of the retinol moiety. Representative images are shown in Fig. 7A and B and lipid droplet quantifications are shown in Fig. 7C–F. Lipid droplets

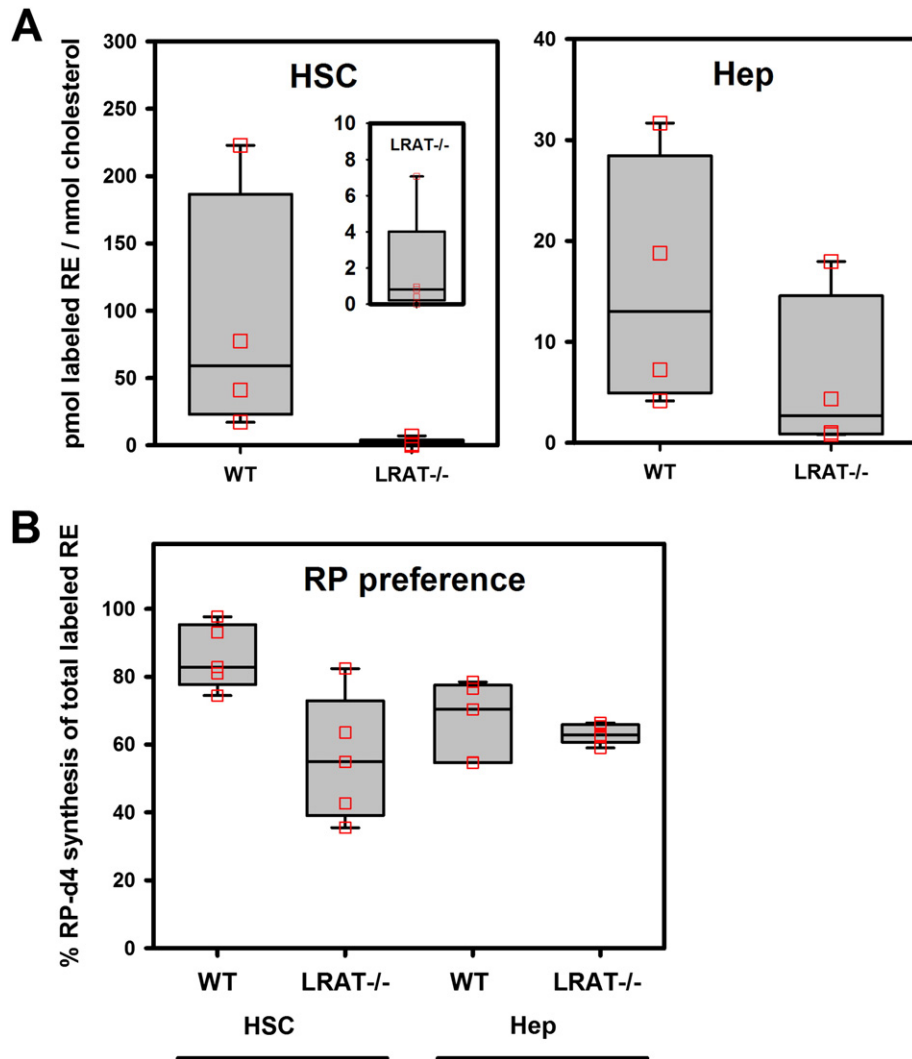


Fig. 5. Retinyl ester synthesis in isolated hepatic stellate cells and hepatocytes from wild type and LRAT knockout mice. (A) Hepatic stellate cells and hepatocytes were isolated from wild type and LRAT^{-/-} mice and plated for 24 h. Retinol (8 μ M) and fatty acids (D₄-palmitate and D₂-oleate 80 μ M each) were then added to the medium. After 24 h, the medium was removed, cells were washed twice with ice-cold PBS and cells were collected. Retinyl ester synthesis was quantified by HPLC-MS as described in [Materials and methods](#). Results shown are from 4 wild type mice and 5 LRAT KO mice. Vertical box plots show the median, the 25th and 75th percentile boundaries of the box and the 10th and 90th percentile boundaries (error bars). The inset shows the same data obtained with LRAT^{-/-} HSCs but with an expanded y-axis (B) quantification of the preference of retinyl palmitate synthesis (D₄-retinyl palmitate: (D₄-retinyl palmitate + D₂-retinyl oleate) \times 100%). Only a very small percentage of the RE-synthesis capacity in the hepatocyte fraction (1.1%) is derived from contaminating HSCs, as determined by the percentage of contaminating HSC cells in the hepatocyte fraction and the amount of cholesterol/number of cells in each fraction (see [Materials and methods](#)).

are observed in HSCs from both wild type and LRAT^{-/-} mice at the earliest possible time point (2 h) after plating the cells ([Fig. 7A](#)). In agreement with our HPLC-MS data (Suppl. Fig. 2) HSCs from wild type mice showed auto-fluorescence, whereas no auto-fluorescence could be detected in HSCs from LRAT^{-/-} mice. The auto-fluorescence signal in HSCs of control mice overlapped with the LD540 signal, showing storage of retinyl esters in lipid droplets. On average, wild type HSCs contain 20.9 ± 13.7 lipid droplets/cell ([Fig. 7C](#)). LRAT^{-/-} HSCs also contain lipid droplets, but less than wild type HSCs (4.3 ± 1.9 /cell). The absence of LRAT also has an effect on the size distribution of lipid droplets in HSCs and as a result the average lipid droplet diameter. LRAT^{-/-} HSCs contain predominantly small lipid droplets with $50.5 \pm 9.0\%$ of the lipid droplets smaller than 700 nm diameter and $30.3 \pm 8.7\%$ of the lipid droplets with a 700–1400 nm diameter ([Fig. 7D](#)). Wild type HSCs also contain lipid droplets with a diameter of 1400–2100 nm ($25.6 \pm 1.4\%$) and the presence of these type of lipid droplets is strongly reduced in LRAT^{-/-} HSCs ($6.5 \pm 1.6\%$, $p \leq 0.05$ Student's *t*-test). As a result, the average lipid droplet size in LRAT^{-/-} HSCs is significantly smaller than in wild type HSCs (medians of 1080 nm and 1618 nm, respectively,

$p \leq 0.001$ Mann-Whitney *U* test) ([Fig. 7E](#)). After 24 h of plating the primary cells ([Fig. 7B](#)), the lipid droplet content drastically increased both in LRAT^{-/-} HSCs (55.0 ± 20.0 lipid droplets/cell) and in wild type HSCs (59.9 ± 42.1 lipid droplets/cell), unambiguously showing the capacity of HSCs to generate lipid droplets in the absence of LRAT ([Fig. 7C](#)). Under these conditions, the average diameter of the lipid droplets ([Fig. 7E](#)) as well as the lipid droplet size distribution ([Fig. 7F](#)) is not significantly different anymore between LRAT^{-/-} HSCs and wild type HSCs. In both cases predominantly small lipid droplets accumulate in the cells and the average lipid droplet diameter decreases. In wild type HSCs the median of the lipid droplet size changes from 1618 nm after to 1020 nm after 24 h incubation. In LRAT KO HSCs the median of the lipid droplet size changes from 1079 nm after to 847 nm after 24 h incubation.

4. Discussion

LRAT is believed to account for the major if not only enzymatic activity involved in liver retinyl ester formation. Indeed, we could not detect

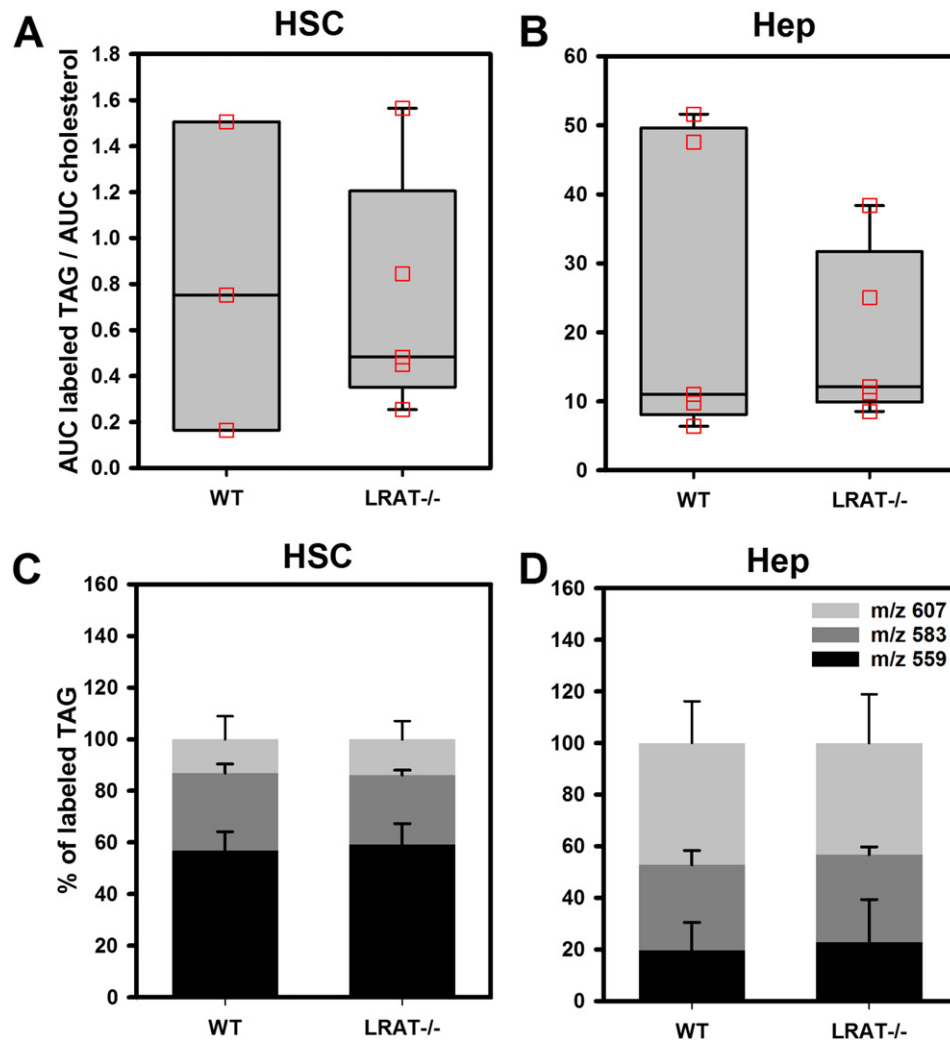


Fig. 6. Triacylglycerol synthesis in isolated hepatic stellate cells and hepatocytes from wild type and LRAT knockout mice. Hepatic stellate cells and hepatocytes were isolated from 4 wild type and 5 LRAT^{-/-} mice and plated for 24 h. Retinol (8 μ M) and fatty acids (D₄-palmitate and D₂-oleate 80 μ M each) were then added to the medium. After 24 h the medium was removed, cells were washed twice with ice-cold PBS and cells were collected. Analysis of labeled triacylglycerol species was performed by HPLC-MS as described in [Materials and methods](#). In all panels, the most prominently labeled TAG species are shown; these TAG species contain the following DAG fragments: m/z 559, DAG D₄-16:0/D₄-16:0; m/z 583, DAG D₄-16:0/D₂-18:1; m/z 607, DAG D₂-C18:1/D₂-C18:1. Panels A and B; triacylglycerol synthesis in HSCs (panel A) and hepatocytes (panel B). Vertical box plots show the median, the 25th and 75th percentile boundaries of the box and the 10th and 90th percentile boundaries (error bars). Panels C and D; TAG species distribution of the three most prominently labeled TAG species (indicated above) in HSCs (panel C) and hepatocytes (panel D). Results are the mean \pm SEM.

retinyl esters in livers of LRAT^{-/-} mice as previously observed by others [13,16,29,38]. Our other data also support the notion that LRAT is the predominant enzyme synthesizing retinyl esters in HSCs *in vivo*. However, upon deletion of the LRAT gene, the retinyl ester synthesis capacity of HSCs was not entirely eliminated and LRAT^{-/-} HSCs retain the capacity to synthesize retinyl esters with a different retinyl ester species distribution.

4.1. Contribution of DGAT1 to retinyl ester synthesis in (activated) HSCs

Retinyl ester synthesis in LRAT-deficient HSCs likely occurs via DGAT1, which is expressed in HSCs [16,27,39]. DGAT1 expression might even be increased in the absence of LRAT [39], although this could not be confirmed in LRAT-deficient mice [16]. Recently we showed an involvement of DGAT1 in the turnover of newly synthesized triacylglycerols in HSCs [27]. Here, evidence for the involvement of DGAT1 in retinyl ester synthesis is presented by taking advantage of the different substrate preferences of DGAT1 and LRAT. LRAT catalyzes the trans-esterification of retinol with an acyl group obtained from the *sn*-1 position of phosphatidylcholine [9–11]. At the *sn*-1 position, PC

carries mostly saturated fatty acids, with palmitic acid and stearic acid being the most abundant species, as determined with specific phospholipases [40–42] or by lipidomic analyses [43,44]. As a result, retinyl palmitate and retinyl stearate are the most abundant retinyl esters synthesized by the LRAT enzyme. In contrast, DGAT1 esterifies retinol using acyl-CoA pools in the cells, which are derived from free fatty acids [45,46]. DGAT1 has a broad fatty acyl-CoA substrate specificity and a variety of retinyl esters are synthesized, including retinyl esters containing unsaturated fatty acids such as retinyl oleate [47]. LRAT and DGAT1 are both present in quiescent HSCs, but LRAT is the predominant enzyme responsible for retinyl ester synthesis as retinyl palmitate is the most abundant species recovered in liver as well as in isolated HSCs ([48] and Fig. 2). Upon HSC activation, LRAT expression is strongly reduced [37] and DGAT1 is the predominant enzyme available for generation of retinyl esters. Indeed, the involvement of DGAT1 in the capacity of activated HSCs to synthesize retinyl esters is supported by our findings on the HSC cell line LX-2 (Figs. 1–3). In addition, activated primary stellate cells synthesize a larger variety of retinyl esters as compared to quiescent primary hepatic stellate cells (Fig. 4), further supporting a role of DGAT1 in activated stellate cells.

4.2. Absence of retinyl esters in HSCs in vivo versus presence of retinyl esters in HSCs in vitro

Despite the presence of DGAT1 in liver stellate cells and their capacity to synthesize retinyl esters as indicated in this study, livers and HSCs from $LRAT^{-/-}$ mice do not contain or only show trace levels of retinyl esters (Table 1; Fig. 5) [13,16,29,38]. Indeed, Yuen et al. recently studied retinyl ester formation in DGAT-deficient mice and showed that DGAT1 does not contribute to retinyl ester formation in the liver [49]. The reason for the lack of retinyl ester storage in $LRAT^{-/-}$ HSCs, despite their synthesizing capacity, is not clear. A possible explanation that may contribute to this phenotype is a disturbed absorption of vitamin A and as a result a reduced supply of vitamin A in the form of chylomicron remnants to hepatocytes and hence HSCs in $LRAT^{-/-}$ mice. $LRAT$ -deficient mice have only 50–60% of the intestinal absorption efficiency of wild type mice when challenged with a physiological dose of retinol [13]. Moreover, ~60% of the retinoid absorbed in chylomicrons of $LRAT$ -deficient mice is as un-esterified retinol, and not as retinyl ester.

4.3. Retinyl ester synthesis in hepatocytes

Deletion of the $LRAT$ gene in mice does affect the retinyl ester synthesizing capacity of isolated hepatocytes. Hepatocytes isolated from wild type (14 pmol labeled REs/nmol cholesterol) or from $LRAT^{-/-}$ mice (3 pmol labeled REs/nmol cholesterol) have a low retinyl ester synthesis capacity as compared to HSCs. Hepatocytes were previously reported not to express $LRAT$ [39,50]. In addition, HSC-contamination ($3.1 \pm 1.9\%$) in the hepatocyte fraction can only explain 1.1% of the measured labeled RE (see legend to Fig. 5). Hence, HSC contamination of the hepatocyte fraction would result in a negligible decrease of labeled REs due to a direct effect of $LRAT$ knockout in HSCs. Moreover, the ratio D_4 -palmitate retinyl ester: (D_4 -palmitate + D_2 -oleate retinyl esters) in hepatocytes did not shift significantly upon deletion of the $LRAT$ gene (one-way ANOVA). Together, these three points suggest that deletion of the $LRAT$ gene in HSCs has some indirect effects on (neighboring) hepatocytes, e.g. due to the lack of retinoid signaling molecules, resulting in a reduction of retinyl ester synthesis (Fig. 5).

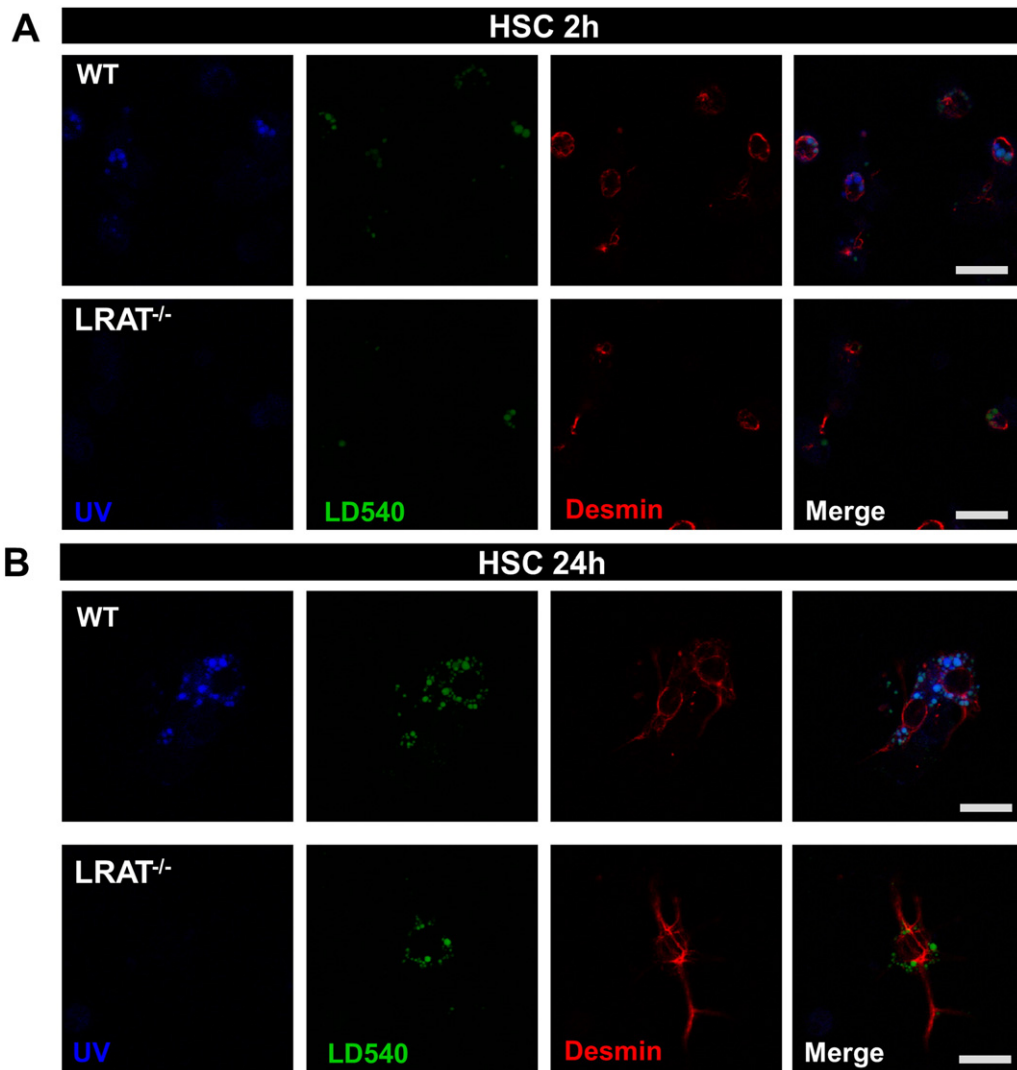


Fig. 7. Identification of retinyl ester and lipid droplet content of hepatic stellate cells and hepatocytes by confocal microscopy. HSCs and hepatocytes were isolated from wild type and $LRAT^{-/-}$ mice as described in Materials and methods. After isolation, cells were plated onto glass coverslips in DMEM/0.5% FBS and after various times, incubations were stopped, the cells fixed in paraformaldehyde and analyzed by confocal microscopy as described in Materials and methods (Panels A and B, scale bars are 20 μm). Lipid droplets were analyzed in desmin-positive cells (HSCs) under the conditions indicated in the figure and as described in Supplementary Table 2. Quantification of lipid droplet characteristics was performed using CellProfiler v2.1.1 (Panels C–F).

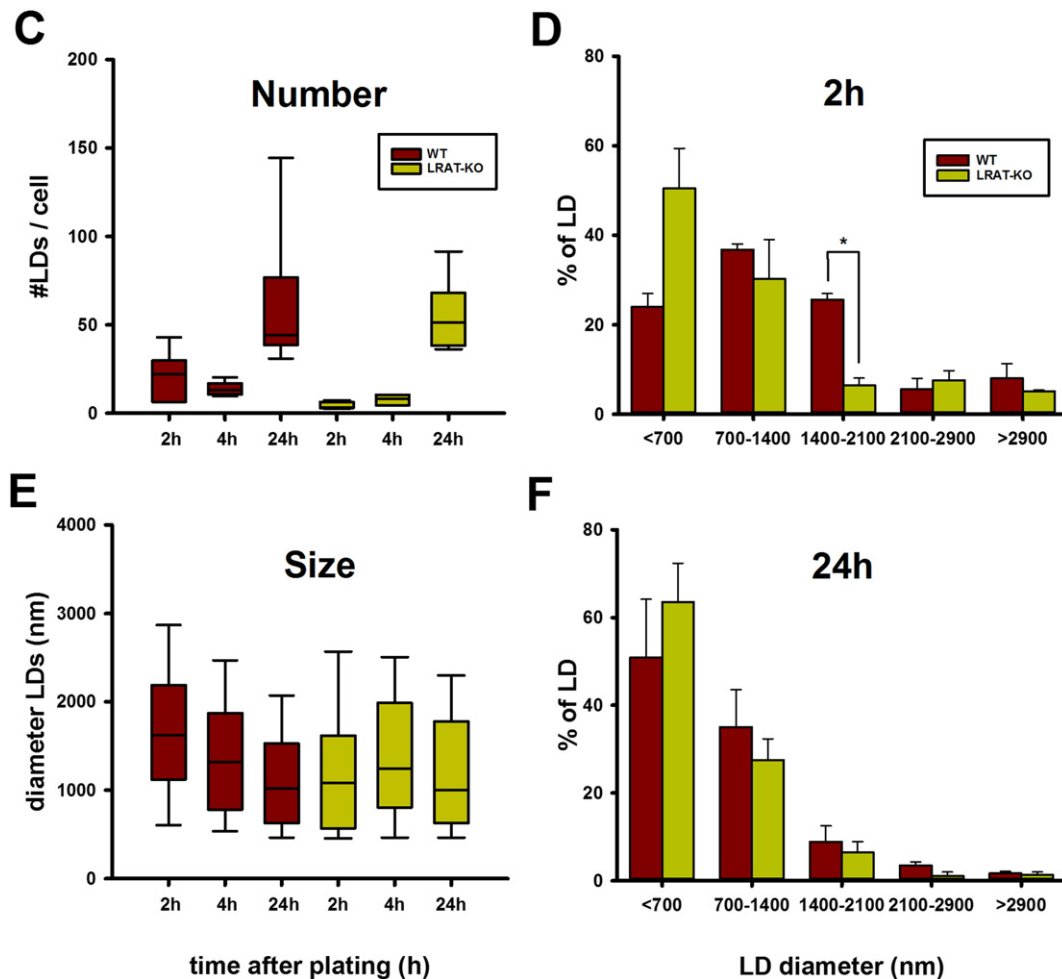


Fig. 7 (continued).

4.4. Lipid droplets in HSCs

Morphological observations show that $LRAT^{-/-}$ HSCs lack lipid droplets that are required for storage of neutral lipids [13]. This is surprising as most cells are capable of storing neutral lipids such as triacylglycerols and cholesteryl esters in the absence of retinyl esters [19–21]. In agreement with this, we show here that HSCs isolated from $LRAT$ knockout mice have the machinery to synthesize triacylglycerols (Fig. 6) and have morphologically distinct lipid droplets in cell culture (Fig. 7). These lipid droplets do not contain retinyl esters, as confirmed by the absence of auto-fluorescence. These data show that $LRAT$ -deficient HSCs have the intrinsic capacity to make lipid droplets. This is further demonstrated by the strong increase in the number of lipid droplets upon 24 h incubation of $LRAT^{-/-}$ HSCs. In addition, lipid droplet formation does not require retinyl ester synthesis as HSCs form lipid droplets in the absence of exogenous retinol, i.e. in the absence retinyl ester synthesis. Thus, neither the $LRAT$ enzyme itself nor its enzymatic activity is required for lipid droplet formation in hepatic stellate cells. $LRAT$ does, however, affect the lipid droplet size and number. Therefore, it seems likely that $LRAT$ has a catalytic effect on lipid droplet formation and maturation. As $LRAT$ expression is strongly reduced in activated HSCs [37], our results may also explain the absence of large lipid droplets in these cells, despite their triacylglycerol and retinyl ester synthesizing capacity.

After 24 h of incubation of primary wild type and $LRAT^{-/-}$ HSCs, the number, the average size distribution, and the average diameter of lipid droplets become indistinguishable between the wild type and knockout

HSCs. This raises the intriguing question why this phenomenon is not happening in vivo and why $LRAT^{-/-}$ HSCs remain devoid of lipid droplets, despite the presence of sufficient levels of fatty acids and retinol in the serum [13] and their capacity to synthesize both triacylglycerols and retinyl esters. The abundance of lipid droplets depends on a balance between synthesis and breakdown of triacylglycerols. Given the fact that the triacylglycerol synthesizing capacity in $LRAT$ -deficient HSCs is fairly normal as compared to wild type HSCs, we suggest that the triacylglycerol hydrolysis rate is enhanced and/or that neutral lipids are stored only in small lipid droplets. Small lipid droplets have a larger surface-to-volume ratio, making them more susceptible to lipases acting at the lipid droplet surface. This would imply that the presence of retinyl esters in lipid droplets indirectly affect the triacylglycerol content by protecting triacylglycerol species from hydrolysis.

Transparency Document

The [Transparency document](#) associated with this article can be found in the online version.

Acknowledgements

The authors would like to thank Dr. C. Thiele (Bonn, Germany) for providing LD540, Dr. Friedman (New York, NY, USA) for donating the LX-2 cell line and Dr. L. Gudas (Cornell University, New York, NY, USA) for providing the $LRAT^{-/-}$ mice. This work was supported by the Seventh Framework Programme of the EU-funded “LipidomicNet”

project (proposal number 202272) to JBH and by a scholarship from the Government of Malaysia (KPT(BS)811221145457) to MA.

Appendix A. Supplementary data

Supplementary data to this article can be found online at <http://dx.doi.org/10.1016/j.bbailip.2016.10.013>.

References

- [1] D.N. D'Ambrosio, R.D. Clugston, W.S. Blaner, Vitamin A metabolism: an update, *Nutrients* 3 (2011) 63–103.
- [2] L.J. Gudas, Emerging roles for retinoids in regeneration and differentiation in normal and disease states, *Biochim. Biophys. Acta* 1821 (2012) 213–221.
- [3] N. Noy, Between death and survival: retinoic acid in regulation of apoptosis, *Annu. Rev. Nutr.* 30 (2010) 201–217.
- [4] W.S. Blaner, J.A. Olson, Retinol and retinoic acid metabolism, in: M.B. Sporn, A.B. Roberts, W.S. Blaner (Eds.), *Retin. Biol. Chem. Med.*, Raven Press, New York 1994, pp. 229–255.
- [5] R. Blomhoff, M.H. Green, J.B. Green, T. Berg, K.R. Norum, Vitamin A metabolism: new perspectives on absorption, transport, and storage, *Physiol. Rev.* 71 (1991) 951–990.
- [6] D.W. Goodman, H.S. Huang, T. Shiratori, Tissue distribution and metabolism of newly absorbed vitamin A in the rat, *J. Lipid Res.* 6 (1965) 390–396.
- [7] S.M. O'Byrne, W.S. Blaner, Retinol and retinyl esters: biochemistry and physiology, *J. Lipid Res.* 54 (2013) 1731–1743.
- [8] H. Senoo, N. Kojima, M. Sato, Vitamin A-storing cells (stellate cells), *Vitam. Horm.* 75 (2007) 131–159.
- [9] P.N. MacDonald, D.E. Ong, Evidence for a lecithin-retinol acyltransferase activity in the rat small intestine, *J. Biol. Chem.* 263 (1988) 12478–12482.
- [10] P.N. MacDonald, D.E. Ong, A lecithin:retinol acyltransferase activity in human and rat liver, *Biochem. Biophys. Res. Commun.* 156 (1988) 157–163.
- [11] J.C. Saari, D.L. Bredberg, Lecithin:retinol acyltransferase in retinal pigment epithelial microsomes, *J. Biol. Chem.* 264 (1989) 8636–8640.
- [12] H. Horchani, S. Bussi eres, L. Cantin, M. Lhor, J.-S. Lalibert -Gemme, R. Breton, C. Salesse, Enzymatic activity of lecithin:retinol acyltransferase: a thermostable and highly active enzyme with a likely mode of interfacial activation, *Biochim. Biophys. Acta* 1844 (2014) 1128–1136.
- [13] S.M. O'Byrne, N. Wongsirirot, J. Libien, S. Vogel, I.J. Goldberg, W. Baehr, K. Palczewski, W.S. Blaner, Retinol absorption and storage is impaired in mice lacking lecithin:retinol acyltransferase (LRAT), *J. Biol. Chem.* 280 (2005) 35647–35657.
- [14] M.D. Orland, K. Anwar, D. Cromley, C.-H. Chu, L. Chen, J.T. Billheimer, M.M. Hussain, D. Cheng, Acyl coenzyme A dependent retinol esterification by acyl coenzyme A: diacylglycerol acyltransferase 1, *Biochim. Biophys. Acta* 1737 (2005) 76–82.
- [15] C.-L.E. Yen, M. Monetti, B.J. Burri, R.V. Farese, The triacylglycerol synthesis enzyme DGAT1 also catalyzes the synthesis of diacylglycerols, waxes, and retinyl esters, *J. Lipid Res.* 46 (2005) 1502–1511.
- [16] N. Wongsirirot, H. Jiang, R. Piantadosi, K.J.Z. Yang, J. Kluge, R.F. Schwabe, H. Ginsberg, I.J. Goldberg, W.S. Blaner, Genetic dissection of retinoid esterification and accumulation in the liver and adipose tissue, *J. Lipid Res.* 55 (2014) 104–114.
- [17] N. Wongsirirot, R. Piantadosi, K. Palczewski, I.J. Goldberg, T.P. Johnston, E. Li, W.S. Blaner, The molecular basis of retinoid absorption: a genetic dissection, *J. Biol. Chem.* 283 (2008) 13510–13519.
- [18] M.Y.S. Shih, M.A. Kane, P. Zhou, C.L.E. Yen, R.S. Streeper, J.L. Napoli, R.V. Farese, Retinol esterification by DGAT1 is essential for retinoid homeostasis in murine skin, *J. Biol. Chem.* 284 (2009) 4292–4299.
- [19] D.L. Brasaemle, N.E. Wolins, Packaging of fat: an evolving model of lipid droplet assembly and expansion, *J. Biol. Chem.* 287 (2012) 2273–2279.
- [20] A. Pol, S.P. Gross, R.G. Parton, Review: biogenesis of the multifunctional lipid droplet: lipids, proteins, and sites, *J. Cell Biol.* 204 (2014) 635–646.
- [21] T.C. Walther, R.V. Farese, Lipid droplets and cellular lipid metabolism, *Annu. Rev. Biochem.* 81 (2012) 687–714.
- [22] W.S. Blaner, S.M. O'Byrne, N. Wongsirirot, J. Kluge, D.M. D'Ambrosio, H. Jiang, R.F. Schwabe, E.M.C. Hillman, R. Piantadosi, J. Libien, Hepatic stellate cell lipid droplets: a specialized lipid droplet for retinoid storage, *Biochim. Biophys. Acta* 1791 (2009) 467–473.
- [23] H. Moriawaki, W.S. Blaner, R. Piantadosi, D.S. Goodman, Effects of dietary retinoid and triglyceride on the lipid composition of rat liver stellate cells and stellate cell lipid droplets, *J. Lipid Res.* 29 (1988) 1523–1534.
- [24] S.L. Friedman, Hepatic stellate cells: protean, multifunctional, and enigmatic cells of the liver, *Physiol. Rev.* 88 (2008) 125–172.
- [25] N. Testerink, M. Ajat, M. Houweling, J.F. Brouwers, V.V. Pulley, H.-J. van Manen, C. Otto, J.B. Helms, A.B. Vaandrager, Replacement of retinyl esters by polyunsaturated triacylglycerol species in lipid droplets of hepatic stellate cells during activation, *PLoS One* 7 (2012) e34945.
- [26] M. Tuohetahuntala, B. Spee, H.S. Kruitwagen, R. Wubbolds, J.F. Brouwers, C.H. van de Lest, M.R. Molenaar, M. Houweling, J.B. Helms, A.B. Vaandrager, Role of long-chain acyl-CoA synthetase 4 in formation of polyunsaturated lipid species in hepatic stellate cells, *Biochim. Biophys. Acta* 1851 (2015) 220–230.
- [27] M. Tuohetahuntala, M.R. Molenaar, B. Spee, J.F. Brouwers, M. Houweling, A.B. Vaandrager, J.B. Helms, ATGL and DGAT1 are involved in the turnover of newly synthesized triacylglycerols in hepatic stellate cells, *J. Lipid Res.* 57 (2016) 1162–1174.
- [28] L. Xu, A.Y. Hui, E. Albanis, M.J. Arthur, S.M. O'Byrne, W.S. Blaner, P. Mukherjee, S.L. Friedman, F.J. Eng, Human hepatic stellate cell lines, LX-1 and LX-2: new tools for analysis of hepatic fibrosis, *Gut* 54 (2005) 142–151.
- [29] L. Liu, L.J. Gudas, Disruption of the lecithin:retinol acyltransferase gene makes mice more susceptible to vitamin A deficiency, *J. Biol. Chem.* 280 (2005) 40226–40234.
- [30] L. Riccalton-Banks, R. Bhandari, J. Fry, K.M. Shakesheff, A simple method for the simultaneous isolation of stellate cells and hepatocytes from rat liver tissue, *Mol. Cell. Biochem.* 248 (2003) 97–102.
- [31] E.G. Bligh, W.J. Dyer, A rapid method of total lipid extraction and purification, *Can. J. Biochem. Physiol.* 37 (1959) 911–917.
- [32] J. Spandl, D.J. White, J. Peyschl, C. Thiele, Live cell multicolor imaging of lipid droplets with a new dye, LD540, *Traffic. Cph. Den.* 10 (2009) 1579–1584.
- [33] N.B. Ghyselsinck, C. B vik, V. Sapin, M. Mark, D. Bonnier, C. Hindelang, A. Dierich, C.B. Nilsson, H. H kansson, P. Sauv nt, V. Azais-Braesco, M. Frasson, S. Picard, P. Chambon, Cellular retinol-binding protein I is essential for vitamin A homeostasis, *EMBO J.* 18 (1999) 4903–4914.
- [34] T.E. Gundersen, Methods for detecting and identifying retinoids in tissue, *J. Neurobiol.* 66 (2006) 631–644.
- [35] T. Wingerath, D. Kirsch, B. Spengler, R. Kaufmann, W. Stahl, High-performance liquid chromatography and laser desorption/ionization mass spectrometry of retinyl esters, *Anal. Chem.* 69 (1997) 3855–3860.
- [36] K. Galler, F. Schleser, E. Fr hlich, R.P. Requardt, A. Kortgen, M. Bauer, J. Popp, U. Neugebauer, Exploitation of the hepatic stellate cell Raman signature for their detection in native tissue samples, *Integr. Biol. Quant. Biosci. Nano Macro* 6 (2014) 946–956.
- [37] J. Kluge, N. Wongsirirot, J.S. Troeger, G.-Y. Gwak, D.H. Dapito, J.-P. Pradere, H. Jiang, M. Siddiqi, R. Piantadosi, S.M. O'Byrne, W.S. Blaner, R.F. Schwabe, Absence of hepatic stellate cell retinoid lipid droplets does not enhance hepatic fibrosis but decreases hepatic carcinogenesis, *Gut* 60 (2011) 1260–1268.
- [38] M.L. Batten, Y. Imanishi, T. Maeda, D.C. Tu, A.R. Moise, D. Bronson, D. Possin, R.N. Van Gelder, W. Baehr, K. Palczewski, Lecithin-retinol acyltransferase is essential for accumulation of all-trans-retinyl esters in the eye and in the liver, *J. Biol. Chem.* 279 (2004) 10422–10432.
- [39] K. Yamaguchi, L. Yang, S. McCall, J. Huang, X.X. Yu, S.K. Pandey, S. Bhanot, B.P. Monia, Y.-X. Li, A.M. Diehl, Diacylglycerol acyltransferase 1 anti-sense oligonucleotides reduce hepatic fibrosis in mice with nonalcoholic steatohepatitis, *Hepatology* 47 (2008) 625–635.
- [40] A. Kuksis, W.C. Breckenridge, L. Marai, O. Stachnyk, Molecular species of lecithins of rat heart, kidney, and plasma, *J. Lipid Res.* 10 (1969) 25–32.
- [41] A. Montfoort, L.M. van Golde, L.L. van Deenen, Molecular species of lecithins from various animal tissues, *Biochim. Biophys. Acta* 231 (1971) 335–342.
- [42] H. Yabuuchi, J.S. O'Brien, Positional distribution of fatty acids in glycerophosphatides of bovine gray matter, *J. Lipid Res.* 9 (1968) 65–67.
- [43] K. Kroos, C.S. Ejising, U. Bahr, M. Karas, K. Simons, A. Shevchenko, Charting molecular composition of phosphatidylcholines by fatty acid scanning and ion trap MS3 fragmentation, *J. Lipid Res.* 44 (2003) 2181–2192.
- [44] H. Kanishchi, Y. Iida, T. Shimizu, R. Taguchi, Separation and quantification of sn-1 and sn-2 fatty acid positional isomers in phosphatidylcholine by RPLC-ESI/MS, *J. Biochem. (Tokyo)* 147 (2010) 245–256.
- [45] Q. Liu, R.M.P. Siloto, R. Lehner, S.J. Stone, R.J. Weselake, Acyl-CoA:diacylglycerol acyltransferase: molecular biology, biochemistry and biotechnology, *Prog. Lipid Res.* 51 (2012) 350–377.
- [46] C.-L.E. Yen, S.J. Stone, S. Koliwad, C. Harris, R.V. Farese, Thematic review series: glycerolipids DGAT enzymes and triacylglycerol biosynthesis, *J. Lipid Res.* 49 (2008) 2283–2301.
- [47] A.C. Ross, Retinol esterification by mammary gland microsomes from the lactating rat, *J. Lipid Res.* 23 (1982) 133–144.
- [48] H.F. Hendriks, W.A. Verhoofstad, A. Brouwer, A.M. de Leeuw, D.L. Knook, Perinatal fat-storing cells are the main vitamin A storage sites in rat liver, *Exp. Cell Res.* 160 (1985) 138–149.
- [49] J.J. Yuen, S.-A. Lee, H. Jiang, P.-J. Brun, W.S. Blaner, DGAT1-deficiency affects the cellular distribution of hepatic retinoid and attenuates the progression of CCl4-induced liver fibrosis, *Hepatobiliary Surg. Nutr.* 4 (2015) 184–196.
- [50] I. Mederacke, C.C. Hsu, J.S. Troeger, P. Huebener, X. Mu, D.H. Dapito, J.-P. Pradere, R.F. Schwabe, Fate tracing reveals hepatic stellate cells as dominant contributors to liver fibrosis independent of its aetiology, *Nat. Commun.* 4 (2013) 2823.
- [51] R.F. Chen, Removal of fatty acids from serum albumin by charcoal treatment, *J. Biol. Chem.* 242 (1967) 173–181.
- [52] S.H. Ganji, S. Tavintharan, D. Zhu, Y. Xing, V.S. Kamanna, M.L. Kashyap, Niacin noncompetitively inhibits DGAT2 but not DGAT1 activity in HepG2 cells, *J. Lipid Res.* 45 (2004) 1835–1845.
- [53] R.J. Barry, F.J. Ca ada, R.R. Rando, Solubilization and partial purification of retinyl ester synthetase and retinoid isomerase from bovine ocular pigment epithelium, *J. Biol. Chem.* 264 (1989) 9231–9238.